This article was downloaded by: [Renmin University of China]
On: 13 October 2013, At: 10:52
Publisher: Taylor & Francis
Informa Ltd Registered in England and Wales Registered Number: 1072954 Registered office: Mortimer House, 37-41 Mortimer Street, London W1T 3JH, UK

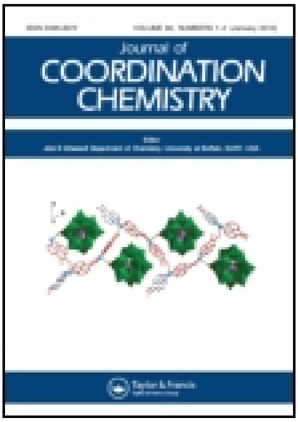

Journal of Coordination Chemistry
Publication details, including instructions for authors and subscription information:
http://www.tandfonline.com/loi/gcoo20

Two supramolecular isomers with different structural features: reversible transformation and fluorescence properties

Guanglu Li [a], Chunlei Wang [b] & Xia Zhang [a]

[a] Department of Chemistry, College of Science, Northeast University, Shenyang, P.R. China

[b] The Library of Northeast Normal University, Changchun, China

Accepted author version posted online: 01 Feb 2013.Published online: 25 Mar 2013.

To cite this article: Guanglu Li, Chunlei Wang & Xia Zhang (2013) Two supramolecular isomers with different structural features: reversible transformation and fluorescence properties, Journal of Coordination Chemistry, 66:7, 1107-1117, DOI: 10.1080/00958972.2013.771776

To link to this article: http://dx.doi.org/10.1080/00958972.2013.771776

PLEASE SCROLL DOWN FOR ARTICLE

Taylor & Francis makes every effort to ensure the accuracy of all the information (the "Content") contained in the publications on our platform. However, Taylor & Francis, our agents, and our licensors make no representations or warranties whatsoever as to the accuracy, completeness, or suitability for any purpose of the Content. Any opinions and views expressed in this publication are the opinions and views of the authors, and are not the views of or endorsed by Taylor & Francis. The accuracy of the Content should not be relied upon and should be independently verified with primary sources of information. Taylor and Francis shall not be liable for any losses, actions, claims, proceedings, demands, costs, expenses, damages, and other liabilities whatsoever or howsoever caused arising directly or indirectly in connection with, in relation to or arising out of the use of the Content.

This article may be used for research, teaching, and private study purposes. Any substantial or systematic reproduction, redistribution, reselling, loan, sub-licensing, systematic supply, or distribution in any form to anyone is expressly forbidden. Terms &

Journal of Coordination Chemistry, 2013
http://dx.doi.org/10.1080/00958972.2013.771776

Taylor & Francis
Taylor & Francis Group

Two supramolecular isomers with different structural features: reversible transformation and fluorescence properties

GUANGLU LI†, CHUNLEI WANG‡ and XIA ZHANG*†

†Department of Chemistry, College of Science, Northeast University, Shenyang, P.R. China
‡The Library of Northeast Normal University, Changchun, China

(*Received 30 March 2012; in final form 26 October 2012*)

Two supramolecular isomers, $\{[Cd_2(pda)_2(1,10'\text{-phen})_2]\cdot H_2O\}_n$ (**1**) and $\{[Cd_2(pda)_2(1,10'\text{-phen})_2]\cdot 4H_2O\}_n$ (**2**) (1,10′-phen = 1,10-phenanthroline, pda = phenylenediacrylate dianion), have been synthesized and characterized by single-crystal X-ray analysis. Complex **1** exhibits a 3D network constructed from 1D rod-shaped secondary building units, while **2** shows a 3D, twofold interpenetrated framework. There exists a reversible transformation between the pair of isomers: when yellow block crystals of **1** are treated under microwave irradiation, colorless plate crystals of **2** are formed; in turn, if crystals of **2** are dissolved in water and left undisturbed about two weeks at room temperature, crystals of **1** reappear. Fluorescence properties of **1** and **2** have also been studied.

Keywords: Coordination polymer; Supramolecular isomer; Reversible transformation; Fluorescence property

1. Introduction

Supramolecular isomerism, the existence of more than one type of supramolecular structure for the same molecular building blocks, has received increasing attention in coordination chemistry and crystal engineering because different isomers differing structural features may result in different physical and chemical properties that lead to various performances when used in molecular adsorption, separation processes, ion exchange, catalysis, sensor technology, and photoelectronics [1–7]. Supramolecular isomerism in coordination polymers, which involves transformation between different isomers, is very important because the process provides opportunities to gain better understanding of factors that influence crystal growth and help to develop new functional materials [8]. Detailed studies on the transformation between supramolecular isomers, however, remain scarce [9, 10].

Compared with coordination polymers constructed from other metal ions, d^{10} coordination polymers are more able to undertake transformations owing to a flexibility to

---

*Corresponding author. Email: xzhang@mail.neu.edu.cn adopt various coordination modes and geometries [11]. Examples of d^{10} coordination polymers have been reported to undergo transformation caused by external stimuli such as light, thermal and other factors [12]. For these coordination polymers, although the conversion processes accompany the breaking of bonds, alteration of oxygen state or loss of guest molecules, crystalline states are retained [13].

Recent studies have demonstrated combining predictable coordination behavior of chelating ligands and the negative charge of a carboxylate have advantages in the crystal engineering of coordination polymers and supramolecular isomers [14]. We have synthesized $\{[Cd_2(pda)_2(1,10'\text{-phen})_2]\cdot H_2O\}_n$ (**1**) and the supramolecular isomer $\{[Cd_2(pda)_2(1,10'\text{-phen})_2]\cdot 4H_2O\}_n$ (**2**). Complex **1** exhibits a 3D network composed of 1D rod-shaped secondary building units (SBUs). The isomer, **2**, shows 3D twofold interpenetration architecture. A reversible transformation exists between the two supramolecular isomers; under microwave irradiation, **1** can transform to **2** and in water at room temperature, **2** can convert to **1**. Fluorescence properties of **1** and **2** have also been studied.

2. Experimental

2.1. *Materials and general methods*

All purchased chemicals were of reagent grade and used without purification. Microwave reactions were performed in a microwave oven (START D, Milestone, maximum power of 1200 W, 2.45 GHz). Elemental analyses (C, H, and N) were performed on a Perkin-Elmer 2400 CHN elemental analyzer. FT/IR spectra were recorded from 4000 to 400 cm^{-1} on an Alpha Centaur FTIR spectrophotometer using KBr pellets. TG analyses were performed on a Perkin-Elmer TGA7 instrument in flowing N_2 with a heating rate of 10 °C min^{-1}. PXRD patterns were recorded on a Siemens D5005 diffractometer with Cu KR ($\lambda = 1.5418$ Å) radiation. Photoluminescence spectra were measured using a FL-2T2 instrument (SPEX, USA) with 450-W xenon lamp monochromated by double grating (1200 gr/mu).

2.2. *Synthesis of 1*

Complex **1** was prepared from $Cd(OAc)_2\cdot 2H_2O$ (0.027 g, 0.1 mmol), H_2pda (0.022 g, 0.1 mmol), 1,10′-phen (0.018 g, 0.1 mmol), and 5 mL H_2O. The mixture was stirred and pH adjusted to 7 with 1 M NaOH. After stirring for another 15 min, the mixture was transferred to a 23-mL Teflon-lined stainless steel bomb and kept at 140 °C under autogenous pressure for four days. The reaction system was cooled to room temperature during 24 h. A large amount of block yellow crystals of **1** were obtained. Yield: 71% (based on Cd). Anal. Calcd for $C_{48}H_{34}N_4O_9Cd_2$: C, 55.67%; H, 3.31%; N, 5.41%. Found: C, 55.54%; H, 3.41%; N, 5.37%. IR (cm^{-1}): 3467 (s), 3382 (s), 1635 (s), 1558 (s), 1419 (s), 1375 (s), 898 (s), 838 (s), 727 (s) (figure S1(a)).

2.3. *Synthesis of 2*

Crystals of **1** (0.10 g) were added to 8 mL of H_2O and the obtained mixture was placed in a 20-mL Teflon autoclave. After heating at 500 W for 20 min, colorless plate crystals of **2** were obtained. Yield: 43% (based on Cd). Anal. Calcd for $C_{48}H_{40}N_4O_{12}Cd_2$: C, 52.91%; H, 3.70%; N, 5.14%. Found: C, 53.07%; H, 3.62%; N, 5.25%. IR (cm^{-1}): 3456 (s), 3060 (m), 1637 (s), 1560 (s), 1515 (s), 1419 (s), 1396 (s), 968 (s), 826 (s), 719 (s) (figure S1(b)).

2.4. *X-ray crystallography*

Suitable single crystals of **1** and **2** were carefully selected under an optical microscope and glued on glass fibers. Structural measurements were performed on a Bruker AXS SMART APEX II CCD diffractometer at 293 K. The structures were solved by the direct method and refined by full-matrix least-squares on F^2 using SHELXTL 97 crystallographic software package and anisotropic thermal parameters were used to refine all nonhydrogen atoms [15, 16]. Carbon-bound hydrogens were placed in geometrically calculated positions; oxygen-bound hydrogens were located in the difference Fourier maps, kept in that position and refined with isotropic temperature factors. Further details of the X-ray structural analysis are given in table 1. Selected bond lengths are listed in table 2. Further details of the crystal structure determination have been deposited to the Cambridge Crystallographic Data Center as supplementary publication. CCDC 842567 and 842568 for **1** and **2** contain the supplementary crystallographic data.

3. Results and discussion

3.1. *Structure description*

Single-crystal X-ray diffraction analysis reveals that **1** is a 3D framework constructed by infinite rod-shaped SBUs and pda linkers. In the fundamental unit, there are two crystallographically independent Cd ions, two pda, two 1,10′-phen, and one free water. Cd1 is a

Table 1. Crystal data and structure refinement results for **1** and **2**.

	1	**2**
Empirical formula	$C_{48}H_{34}N_4O_9Cd_2$	$C_{48}H_{40}N_4O_{12}Cd_2$
Formula weight	1035.59	1089.64
Crystal system	Monoclinic	Monoclinic
Space group	$P2_1/c$	$P2_1/c$
a/Å	11.0512	23.768
b/Å	23.463	18.231
c/Å	15.7410	10.394
β/°	101.882	91.180
V/Å^3	3990.9	4503.2(5)
Z	4	4
D_{calcd}/(g cm^{-3})	1.722	1.607
F (000)	2072	2192
Reflections collected	19,846	24,635
Reflections unique	7013	7922
R (int)	0.0196	0.0246
Data / restraints / parameters	7013 / 11 / 581	7922 / 20 / 651
Goodness-of-fit on F^2	1.027	1.030
R_1 [$I > 2\sigma(I)$]	0.0431	0.0287
wR_2 [$I > 2\sigma(I)$]	0.1453	0.0866
R_1 (all data)	0.0484	0.0353
wR_2 (all data)	0.1532	0.0914

$R_1 = \Sigma||F_o| - |F_c||/\Sigma|F_o|$; $wR_2 = \Sigma[w(F_o^2 - F_c^2)^2]/\Sigma[w(F_o^2)^2]^{1/2}$.

Table 2. Selected bond lengths for **1** and **2**.

1			
Cd(1)–O(7)#1	2.191(3)	Cd(1)–O(1)#3	2.408(3)
Cd(1)–O(3)#2	2.229(3)	Cd(1)–O(6)	2.514(3)
Cd(1)–N(1)	2.455(3)	Cd(1)–N(2)	2.434(3)
Cd(2)–O(2)	2.258(3)	Cd(2)–O(4)#2	2.321(3)
Cd(2)–O(5)	2.435(3)	Cd(2)–O(6)	2.352(3)
Cd(2)–N(3)	2.431(4)	Cd(2)–N(4)	2.347(4)
2			
Cd(1)–O(1)	2.257(18)	Cd(1)–O(3)#2	2.256(18)
Cd(1)–O(4)#2	2.501(2)	Cd(1)–O(7)#1	2.255(2)
Cd(1)–N(1)	2.321(2)	Cd(1)–N(2)	2.392(2)
Cd(2)–O(1)	2.343(18)	Cd(2)–O(2)	2.523(2)
Cd(2)–O(5)	2.462(2)	Cd(2)–O(6)	2.271(19)
Cd(2)–O(8)#1	2.316(2)	Cd(2)–N(3)	2.313(2)
Cd(2)–N(4)	2.388(2)		

Symmetry transformations used to generate equivalent atoms for **1**: #1 $-x$, $y+1/2$, $-z+3/2$; #2 $-x+1$, $y-1/2$, $-z+1/2$; #3 x, $-y+1/2$, $z+1/2$; for **2**: #1 $-x+1$, $y-1/2$, $-z+3/2$; #2 $-x$, $y-1/2$, $-z+½$.

distorted octahedron and connects with four carboxyl oxygen atoms from four pda with Cd–O distances and O–Cd–O angles ranging from 2.191(3) to 2.514(3) Å and 82.72(9) to 168.82(11)°. The other two coordination sites are occupied by 1,10′-phen (figure 1(a)). Cd2 has the same kind of connection as Cd1 but with different bond lengths and angles (figure 1(b)). In **1**, the four carboxylates of two unique pda ligands adopt three different connection modes, resulting in formation of a cadmium-carboxylate chain along the *c* axis (figure 2). The infinite rod-shaped cadmium-carboxylate chain can be regarded as a SBU, where the two independent Cd ions are separated by 3.876 Å. These SBUs are linked in parallel by pda and give a 3D coordination framework. The structure of **1** has channels of 12.13 × 12.13 Å dimensions with a void space running along the *c* axis; the channels are occupied by 1,10′-phen, which coordinate to Cd(1) and Cd(2) (figure 3). Yaghi and others have reported a series of coordination polymers constructed from 1D rod-shaped SBUs [17]. Based on topology theory, **1** exhibits a pcu-type rod packing.

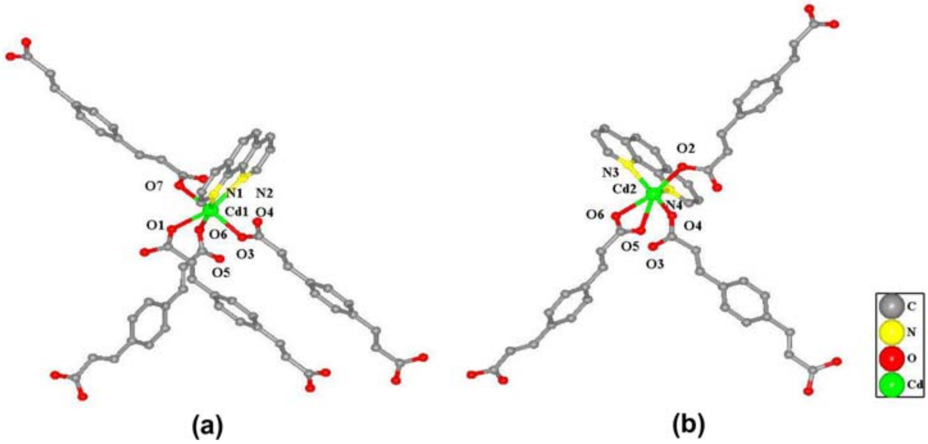

Figure 1. The coordination environments of Cd(1) and Cd(2) in **1**; hydrogens are omitted for clarity.

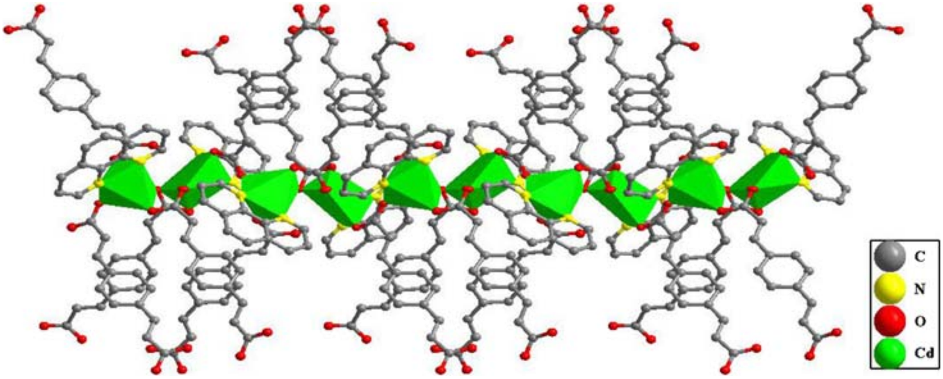

Figure 2. Infinite rod-shaped SBUs used to assemble **1**.

If the guest water molecules are neglected, **2** has the identical molecular formula and chemical components as **1**. Its fundamental unit is also made up of two crystallographically independent Cd ions, two pda and two 1,10′-phen. Cd(1) connects with four carboxyl oxygen atoms from different pda ligands. The Cd–O bond distances range from 2.255(2) to 2.501(2) Å. Two nitrogen atoms from 1,10′-phen occupy the other two coordination sites with an average Cd–N bond distance 2.357 Å. This results in the distorted octahedral coordination mode of Cd(1) (figure 4(a)). Unlike Cd(1), Cd(2) is a distorted pentagonal bipyramidal coordination sphere consisting of five carboxyl oxygen atoms from three different pda and two nitrogen atoms from 1,10′-phen (figure 4(b)). These two Cd ions are bridged by a pair of pda carboxylates into a binuclear Cd unit with the Cd(1)–Cd(2) distance 3.928 Å. Two independent pda ligands have two coordination modes: in the first pda, one carboxylate chelates and another bridges; in the second pda, one carboxylate chelates and the other chelate-bridges. With these connection modes, the adjacent binuclear Cd units are bridged and form a 2D layer with (4, 4) topology (figure 5(a)).

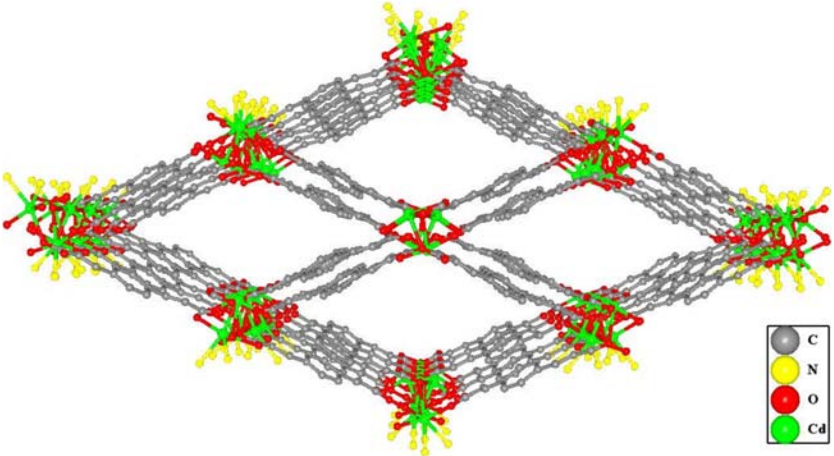

Figure 3. The 3D framework of **1** (1,10′-phen are omitted).

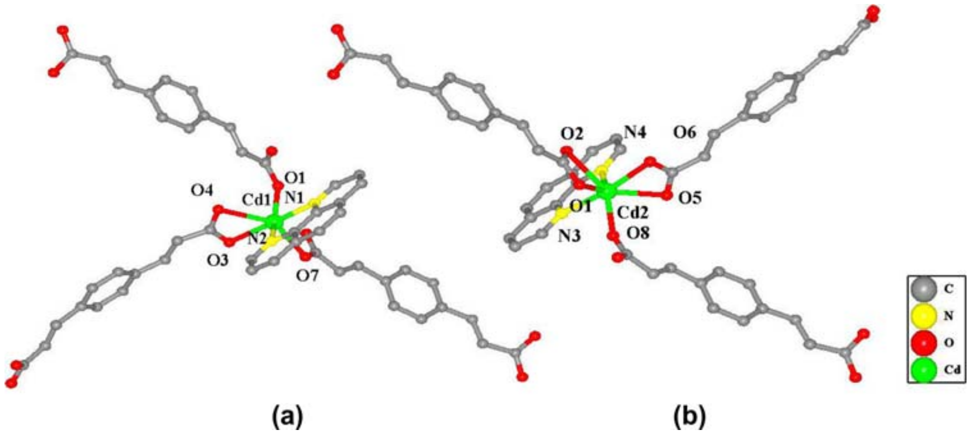

Figure 4. The coordination environments of Cd(1) and Cd(2) in **2**; hydrogens are omitted for clarity.

Different from previously reported 2D layer complexes with (4, 4) topology, the layer structure reported here exhibits 'up' and 'down' arms pointing from both sides of each layer, resulting in the interdigitation of **2** [18, 19]. There are two factors that play important roles in generation of the interdigitated network of **2**: first, four pairs of binuclear Cd units and four pda ligands form a large cavity and second, dangling 1,10′-phen ligands are disposed in a mutual antiorientation and the length of each dangling 1,10′-phen is longer than the distance of adjacent layers. Based on these points, the dangling arms of each layer point into the cavities of neighboring layers in a mutual relationship and each cavity is interdigitated by two arms belonging to two different layers, one entering from one side, while the other from the opposite side (figure 5(b)). These layers are mutually interdigitated to create a stable framework.

In this framework, the separated $[Cd_2(pda)_2(1,10'\text{-phen})_2]_n$ layers stack along the *c* crystal direction and construct a 3D supramolecular network with π–π interactions between 1,10′-phen with distances of neighboring aromatic rings from 3.651 to 3.749 Å and the angle of the aromatic rings is 2.420° (figure 6(a)). So, the binuclear Cd units can be treated as six connected nodes, linking with four binuclear Cd units in the same layer and two binuclear Cd units from two adjacent layers. The connectivity pattern gives a 3D supramolecular network with α-Po topology (figure 6(b)). Owing to the length of pda, the single network is porous. The pore exhibits dimensions of 11.170 × 17.640 Å, which leads to twofold interpenetration structure of **2** (figure 7).

3.2. *Structure transformation between 1 and 2*

The most interesting feature of **1** and **2** is a reversible transformation. After crystals of **1** were placed in a microwave oven and reacted 20 min, colorless plate crystals appeared. The XRPD pattern of these new samples exhibits significant change, which matches well with the pattern of **2** as calculated from the single-crystal X-ray analysis (figure 8(a)). If the crystals of **2** (0.10 g) are placed in 10 mL of H_2O and left undisturbed for two weeks at room temperature, yellow block crystals were found that show similar XRPD pattern to **1** as simulated from single-crystal X-ray data (figure 8(b)).

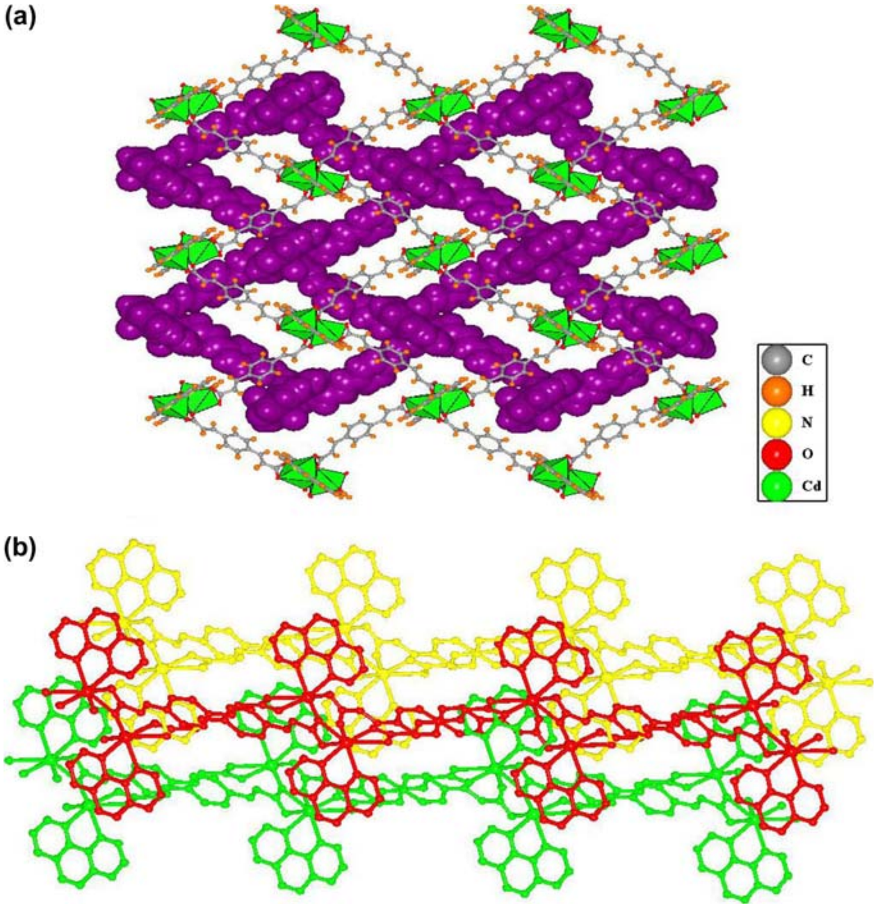

Figure 5. (a) (4, 4) Topology layer of **2** along the *c* axis and (b) the interdigitated structure of **2** along the *b* axis.

Several examples of irreversible transformation between supramolecular isomers have been studied, but reversible transformation has never been reported. Thus, the transformation between **1** and **2** represents the first example [9, 10].

Coordination of pda seems to play an important role in transformation between **1** and **2**. In **1**, the pda adopt two coordination modes. In one type of pda, two carboxylates bridge, while in the second type of pda, one carboxylate chelate-bridges while the other is monodentate. For **2**, one carboxylate of pda is chelating-bridging, while the other chelates. In the second type of pda, one chelates and the other bridges. With the change of the coordination modes of carboxylates, rearrangements of bonds between metal centers occur. During the transformation from **1** to **2**, accompanying the cleavage of three bonds (Cd1–O6, Cd2–O2, and Cd2–O4), three new bonds (Cd1–O1, Cd1–O4, and Cd2–O8) are formed. During these changes, Cd2–O2 bond is the key factor in the transformation process which leads to change of dimensionality and conversion between **1** and **2**.

Conversion between **1** and **2** involves not only formation of new covalent bonds, but also change of dimensionality. Only a few examples have been reported where single-crystal nature of coordination polymers is retained when structural transformations are accompanied with changes of covalent bonds and dimensionality [20].

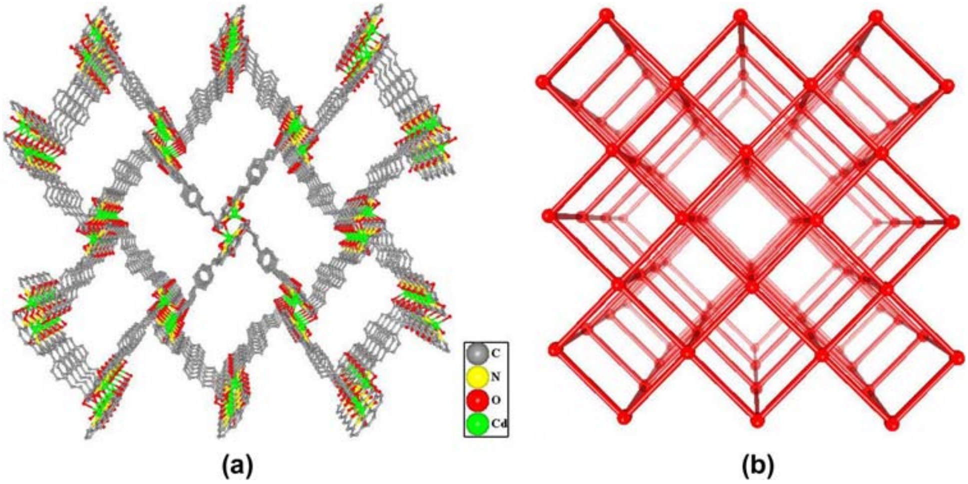

Figure 6. (a) The 3D supramolecular framework of **2** and (b) representation of the α-Po topology of **2**.

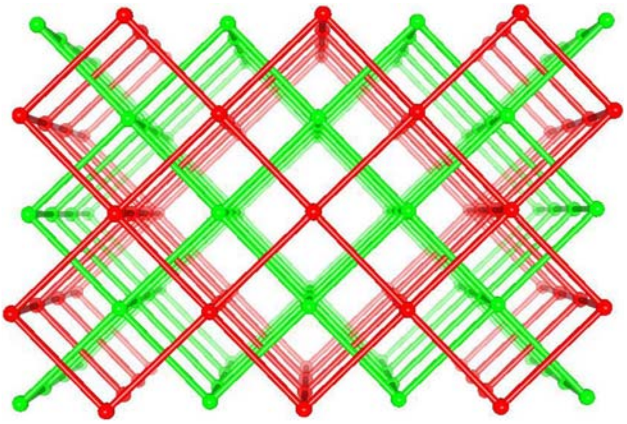

Figure 7. Scheme representation of the 3D twofold interpenetration network of **2**.

3.3. *IR spectroscopy*

For **1**, absorptions at 1635, 1558, and 1419 cm^{-1} display asymmetric and symmetric vibrations, respectively; the separations (Δ) between γ_{asym} (CO_2) and γ_{sym} (CO_2) are 216 and 129 cm^{-1}. The IR spectrum of **2** shows absorptions at 1637, 1560, and 1515 cm^{-1} and the Δ values are 77 and 122 cm^{-1}. For these two complexes, the Δ values are in agreement with the results of the single crystal analysis.

3.4. *Thermal analysis*

To examine stabilities of **1** and **2**, thermal gravimetric analysis (TGA) were carried out in nitrogen atoms from 30 to 800 °C (figure S2). For **1**, the first weight loss of 1.86% at 87–105 °C is due to loss of guest water (calcd. 1.74%). From 313 to 406 °C, weight loss of

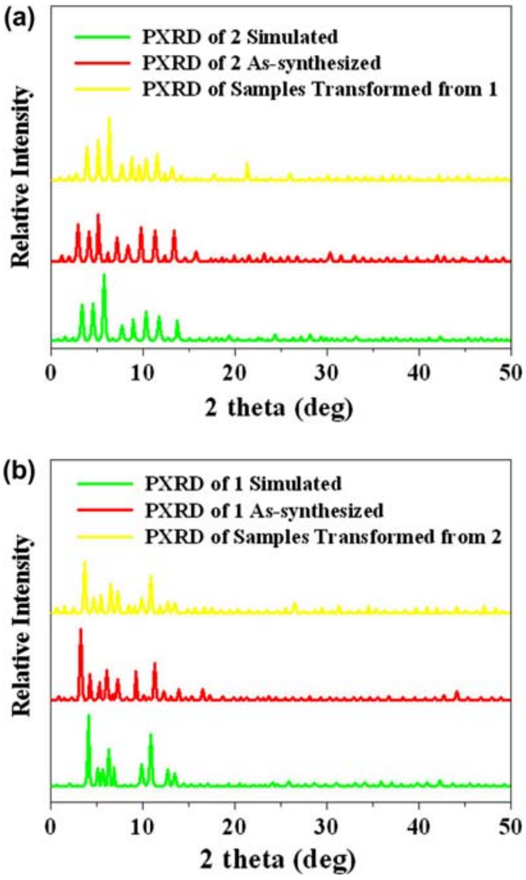

Figure 8. (a) PXRD pattern of **2** and (b) PXRD pattern of **1**.

76.82% should correspond to decomposition of organic ligands (calcd. 76.94%). Complex **2** also displays two-step weight loss, 6.55% from 83 to 112 °C and 73.04% from 307 to 412 °C, respectively, which can be attributed to loss of guest water (calcd. 6.61%) and organic ligands (calcd. 73.13%), respectively. Thermal properties of crystals transformed from **1** have similar TGA curve to **2**. Thermal properties of crystals transformed from **2** give TGA curve similar to **1** (figure S3). These processes further indicate a reversible transformation between **1** and **2**.

3.5. *Fluorescence*

Coordination polymers composed of d^{10} metal centers have fluorescence properties with potential applications in photochemistry, chemical sensors, etc. Fluorescence spectra of free H_2pda, **1,** and **2** were measured at room temperature in the solid state (figure 9). Emission peaks are observed at 426, 408, and 441 nm, respectively (with $\lambda_{ex} = 310$ nm). The emissions of **1** and **2** can be ascribed to π–π^* or π–n transitions of organic ligands [21]. Compared with that of free H_2pda, **1** and **2** exhibit intense emissions at room temperature, attributed to rigidity of their framework [22–24].

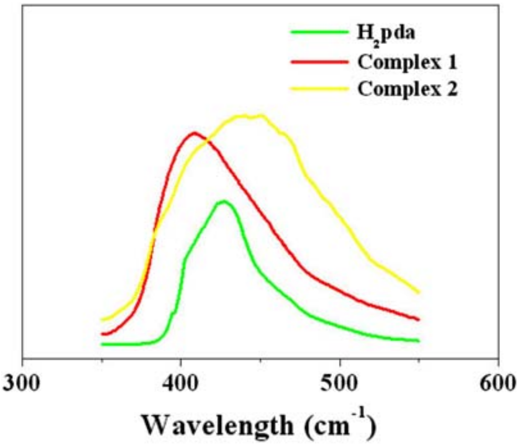

Figure 9. The fluorescence properties of H_2pda, **1,** and **2**.

4. Conclusion

A pair of supramolecular isomers was synthesized with reversible transformation between these two isomers. When treated with microwave irradiation, **1** turns into **2**. After dissolving in water and leaving undisturbed for two weeks, colorless plate crystals of **2** convert to block yellow crystals of **1** slowly. These two complexes exhibit different structural features. Complex **1** shows a 3D network, composed by rod-shaped SBUs, and **2** exhibits a 3D twofold interpenetrated framework. **1** and **2** fluoresce. The reversible transformation between **1** and **2** is a simple conversion phenomenon, paving the way for preparation of new supramolecular isomers unavailable by direct synthesis.

Supplementary material

Crystallographic data for the structural analysis have been deposited with the Cambridge Crystallographic Data Center, CCDC reference numbers: 870430 (**1**), 870431 (**2**).

Acknowledgments

We gratefully acknowledge financial supports from National Natural Science Foundation of China (21103017).

References

[1] J.P. Zhang, X.C. Huang, M.X. Chen. *Chem. Soc. Rev.*, **38**, 2385 (2009).
[2] X.C. Huang, J.P. Zhang, X.M. Chen. *J. Am. Chem. Soc.*, **126**, 13218 (2004).
[3] H.L. Cui, S. Zhan, Z.M. Li, S.W. Ng, D. Li. *Dalton Trans.*, **40**, 6490 (2011).
[4] B. Rather, B. Moulton, R.D.B. Walsh, M.J. Zaworotko. *Chem. Commun.* 694, (2002).
[5] G.P. Yang, L. Hou, Y.Y. Wang, Y.N. Zhang, Q.Z. Shi, S.R. Batten. *Cryst. Growth Des.*, **11**, 936 (2011).
[6] P.X. Yin, J. Zhang, Z.J. Li, Y.Y. Qin, J.K. Cheng, L. Zhang, Q.P. Lin, Y.G. Yao. *Cryst. Growth Des.*, **9**, 4884 (2009).

[7] X.D. Zheng, Y.L. Hua, R.G. Xiong, J.Z. Ge, T.B. Lu. *Cryst. Growth Des.*, **11**, 302 (2011).
[8] D. Braga, F. Grepioni. *Chem. Soc. Rev.*, **29**, 229 (2000).
[9] J.K. Sun, X.H. Jin, C. Chen, J. Zhang. *Inorg. Chem.*, **49**, 7046 (2010).
[10] J.J. Jiang, L. Li, M.H. Lan, M. Pan, A. Eichhöfer, D. Fenske, C.Y. Su. *Chem. Eur. J.*, **16**, 1841 (2010).
[11] A.S. Filatov, O. Hietsoi, Y. Sevryugina, N.N. Gerasimchuk, M.A. Petrukhina. *Inorg. Chem.*, **49**, 1626 (2010).
[12] M.S. Wang, G.C. Guo, W.Q. Zou, W.W. Zhou, Z.J. Zhang, G. Xu, J.S. Huang. *Angew. Chem. Int. Ed.*, **47**, 3565 (2008).
[13] Y.G. Huang, B. Mu, P.M. Schoenecker, C.G. Carson, J.R. Karra, Y. Cai, K.S. Walton. *Angew. Chem. Int. Ed.*, **50**, 436 (2011).
[14] J.P. Zhang, X.M. Chen. *Chem. Commun.* 1869, (2006).
[15] G.M. Sheldrick. *SHELXL97, Program for Crystal Structure Refinement*, University of Göttingen, Germany (1997).
[16] G.M. Sheldrick. *SHELXL97, Program for Crystal Structure Solution*, University of Göttingen, Germany (1997).
[17] X.X. Xu, X. Zhang, X.X. Liu, T. Sun, E.B. Wang. *Cryst. Growth Des.*, **10**, 2272 (2010).
[18] Y. Hijikata, S. Horike, M. Sugimoto, H. Sato, R. Matsuda, S. Kitagawa. *Chem. Eur. J.*, **17**, 5138 (2011).
[19] E.Y. Choi, L.D. Devries, R.W. Novotny, C.H. Hu, W. Choe. *Cryst. Growth Des.*, **10**, 171 (2010).
[20] B. Zhang, D.B. Zhu, Y. Zhang. *Chem. Eur. J.*, **16**, 9994 (2010).
[21] Q. Sun, Q. Yue, J.Y. Zhang, L. Wang, X. Li, E.Q. Gao. *Cryst. Growth Des.*, **9**, 2310 (2009).
[22] G.H. Wang, Z.G. Li, H.Q. Jia, N.H. Hu, W. Xu. *J. Cryst. Growth Des.*, **8**, 1932 (2008).
[23] Q.R. Fang, G.S. Zhu, M. Xue, Q.L. Zhang, J.Y. Sun, X.D. Guo, S.L. Qiu, S.T. Xu, P. Wang, D.J. Wang, Y. Wei. *Chem. Eur. J.*, **12**, 3754 (2006).
[24] Q. Sun, J.Y. Zhang, H. Tian, Y.Q. Wang, E.Q. Gao. *Inorg. Chem. Commun.*, **12**, 426 (2009).